Pore Size Dependent Slippage in Capillary Filling of Compressed Carbon Nanotube Sponges

X. Li[1], Y. Xue[1], M. Zou[2], A. Cao[2] AND H. Duan[1,3,*]

[1]*State Key Laboratory for Turbulence and Complex Systems, Department of Mechanics and Engineering Science, College of Engineering, BIC ESAT, Peking University, Beijing 100871, China*
[2]*Department of Materials Science and Engineering, College of Engineering, Peking University, Beijing 100871, China*
[3]*CAPT, HEDPS and IFSA Collaborative Innovation Center of MoE, Peking University, Beijing 100871, China*

Liquid slippage in nanofluidic systems such as carbon nanotubes has attracted great research interest in the past decade. However, it remains unclear whether liquid slippage can happen in a capillary filling system with wetting surface. In this work, we experimentally demonstrate a capillary slipping flow in compressed carbon nanotube sponges for both oil and water, which shows clear dependence on the effective pore size of the sponge. The slip length reaches around 20 nanometers for our most compressed sponges. The present work may inspire the research on designing nanofluidic devices with wetting surfaces and meanwhile high fluid transport rate.

Keywords: Capillary filling, CNT sponges, liquid slippage, pore-size dependence

1 INTRODUCTION

Capillary filling in porous media has attracted great attention from fundamental research to engineering applications [1-3]. Different capillary filling regimes have been identified, such as linear and square-root (or Lucas-Washburn) regimes, resulting from the compromise among the inertial, gravitational, viscous and capillary forces [4-8]. The filling kinetics also shows

---

significant dependence on the channel size. When it approaches nanometer scale, the surface effect becomes dominated, making the filling process susceptible to the solid-liquid boundary condition [3]. The immobility of strongly pre-adsorbed water monolayers in hydrophilic nanopores could retard the fluidity of water in nanoconfinement, which has been used to rationalize the observation of the classic Lucas-Washburn capillary rise dynamics in nanoporous silica with macroscopic hydrodynamics [9, 10]. On the other hand, pronounced liquid slippage in carbon nanotubes and graphene nanocapillaries has been widely demonstrated by numerical simulations and experiments [11-18]. This inspires the research on how liquid slippage modifies the capillary filling kinetics [19, 20]. However, the existence of liquid slippage on a hydrophilic surface premising the spontaneous capillary action is still under debate [21-25]. Although molecular dynamics simulations have revealed a slip length comparable with the nanochannel size in a capillary flow of polymer melt [26], to the best of our knowledge, few experiments have evidenced such a slip effect in a capillary filling process.

In this work, we take advantage of the compressibility of carbon nanotube (CNT) sponges to investigate the capillary filling kinetics in these sponges with different effective squeezed pore size. CNT sponges are randomly stacked with carbon nanotubes into 3D macroscopic monoliths and exhibit high porosity (> 99%), conductivity and mechanical flexibility [27]. The inter-CNT pore space is adjustable through simple compression (as schematically shown in Figure 1A) without hindering continuous fluid flow [28], making this kind of sponges an ideal platform for studying the dependence of capillary filling kinetics on the effective pore size using a gravimetric method (see Figure 1B). While these sponges show superior ability for oil adsorption due to their intrinsic lipophilicity and hydrophobicity, electrocapillary effects can render them hydrophilic so as to spontaneously imbibe water [29]. Thus, both oil and water are used here to probe the slip boundary condition during capillary filling in carbon nanotube sponges.

2 EXPERIMENTAL PROCEDURES

CNT sponges were fabricated by chemical vapor deposition on a copper wire, resulting in cylindrically shaped samples with diameter of approximately 7 mm (see Figure 1C). The scanning electronic microscopic (SEM) image of an as-grown sponge is shown in Figure 1D, illustrating an assembly of uniformly distributed multi-walled carbon nanotubes. CNT sponges with reduced pore size were obtained by compressing as-grown sponges uniformly in the radial direction using heat shrink tubing under controlled temperature and heating time. Prior to thermal compression, as-grown sponges were covered with a thin, thermally stable PTFE film to avoid sample contamination. This film also gives spatial confinement of sponge samples and helps minimize liquid
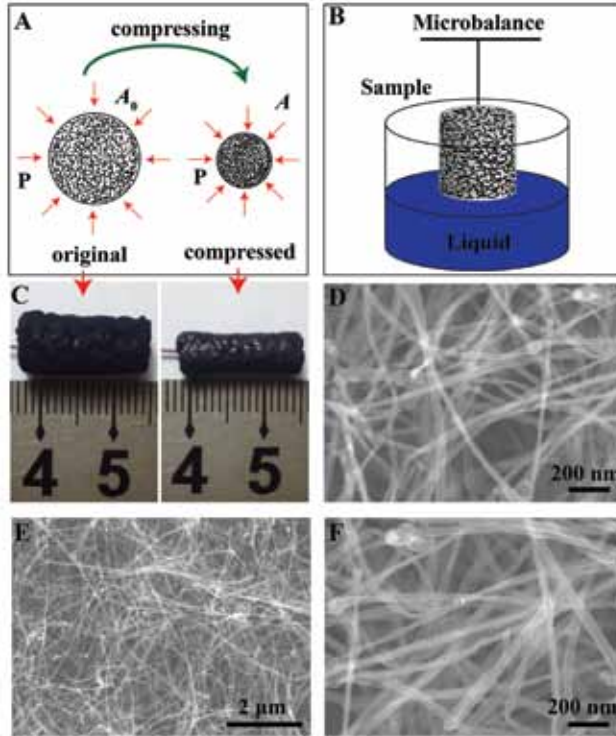
FIGURE 1

Carbon nanotube sponges and experimental setup. (A) Schematics show the compression of CNT sponges in the radial direction by heat shrink tubing. (B) Schematic shows the experimental setup with a sponge sample hung from a microbalance over a liquid reservoir. (C) Photography of as-grown (left) and compressed CNT sponges (right). (D) SEM image of as-grown CNT sponges. (E) and (F) show the SEM images of compressed sponges with lower and higher magnification, respectively.

evaporation from the sidewall. The compression ratio (α) is calculated according to $\alpha = (A_0-A)/A_0$, where A and A_0 are cross-sectional areas of compressed and as-grown sponges, respectively. Here, α ranges from 0 up to around 80% in the present experimental conditions. SEM images in Figure 1E and Figure 1F show the uniform structure of compressed sponges, with only slightly increased packing density of CNTs in comparison with that of as-grown sponges (see Figure 1D).

Gravimetric measurement was used to investigate the spontaneous capillary filling of oil and water in CNT sponges. All experiments were carried out at room temperature (~25°C). Two hydrocarbons with different chain length, that is, cyclohexane (Sigma-Aldrich, Shanghai), melted tetracosane (Sigma-Aldrich, Shanghai) at 80°C, as well as 1 M KOH (Sigma-Aldrich, Shanghai) aqueous solution were used as the imbibed liquid. Their physical properties are listed in Table 1 (cyclohexane and 1 M KOH at 25°C, tetra-

TABLE 1
Physical parameters of cyclohexane, tetracosane and 1M KOH solution.

	Density (g/ml)	Viscosity (mP·s)	Surface Tension (mN/m)
C_6H_{12} [30]	0.778	0.993	24.33
$C_{24}H_{50}$ [30]	0.763	2.859	26.22
1M KOH [31]	1.046	1.054	73.90

cosane at 80°C). In order to initialize the spontaneous imbibition of water, a constant electrode potential of -1.0 V (versus Ag/AgCl in 3 M KCl) was applied on the sponge, which renders the sponge hydrophilic [28]. The sponge sample was hung from a microbalance (ME36S; Sartorius, GmbH) to monitor the imbibed mass variation (Figure 1B). An automatic lab stage was used to raise the liquid level to contact the test sample and start the imbibition.

3 RESULTS AND DISCUSSION

Figure 2 shows the imbibed mass changes (m) of cyclohexane, melted tetracosane and 1 M KOH with time (t) for sponge samples with different compression ratio (α). We remark that abrupt mass change at the contact moment of the sponge with test liquid has been subtracted from the experiment data. A linear correlation between the imbibed mass (m) and the square root of time ($t^{1/2}$) is recovered here for all the three imbibed liquids and sponge compression ratios (α), which clearly indicates the classic Lucas-Washburn law. The plateau of mass change is reached when the sample is saturated with liquid. The saturation value, implying the imbibing capacity of a sponge, decreases with the compression ratio since the inter-CNT space has been reduced. Note that a gradual transition between the Lucas-Washburn filling and the final saturation phases was observed for both experiments using hydrocarbon liquids and aqueous solution. This may be related to the invasion front broadening during imbibition as discussed in Refs. [32] and [33]. The more gradual transition for hydrocarbon experiments may be attributed to their better affinity with CNT sponges. This results in the slight expansion of the free top end of sponge samples after being fully saturated, which is not observed for the case of aqueous solution.

To achieve a better understanding of the imbibition kinetics, we investigate the variation of the imbibition coefficient with the compression degree of CNT sponges for different liquid, that is, the slope (C_m) in the linear mass change with square root of time as shown in Figure 2. According to the Lucas-Washburn equation, the imbibition coefficient (C) is expressed as [31]
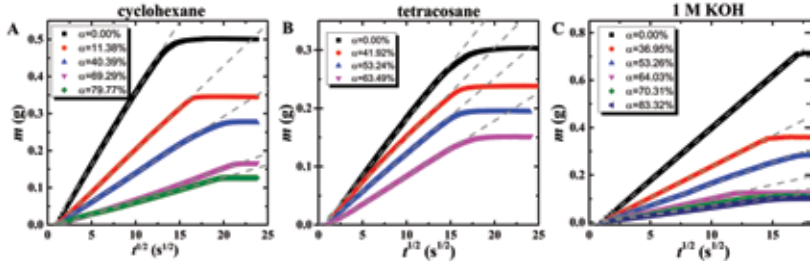
FIGURE 2

Capillary filling in compressed CNT sponges. Graphs show imbibed mass change (m) with square root of time ($t^{1/2}$) for cyclohexane (A), melted tetracosane (B) and 1 M KOH aqueous solution (C), respectively.

$$C = \rho A \phi \sqrt{\frac{r}{\tau} \frac{\sigma \cos \theta}{2\eta}}, \tag{1}$$

where ρ, η, σ, and θ are liquid density, viscosity, surface tension, and contact angle, respectively, and A, ϕ, τ, and r are cross-sectional area, porosity, tortuosity, and effective pore radius of sponge samples. The tortuosity (τ) characterizes the connectivity and meandering of the pores, and for fibrous media, τ is close to 1. The sponge compression may increase τ slightly but generally within 10% in the present experiment condition [34, 35], which only gives slight underestimation of the effective pore radius. Thus, it is a good approximation to assume t equal to 1 and independent of compression. For as-grown sponges, the initial values of porosity and effective pore radius are measured to be 99% and 81 nm (r_0), respectively [28]. We remark that here only the inter-CNT space contributes to the spontaneous imbibition as the inner-CNT space is sealed by catalytic nanoparticles. We estimated the volume fraction of the inter-CNT space or the actual porosity (ϕ_0) of as-grown sponges accounting for liquid imbibition by measuring the total volume of imbibed oil into a sponge sample, which gives ϕ_0 ~ 94%. Then the porosity (ϕ) of a sponge with a compression ratio (α) can be calculated by the following geometric relation,

$$\phi = (\phi_0 - \alpha) / (1 - \alpha). \tag{2}$$

Further geometric calculation gives the expected pore radius of a compressed sponge,

$$r_g = r_0 \sqrt{(\phi_0 - \alpha) / \phi_0}. \tag{3}$$

Here and in the following the subscript "0" means as-grown sponges and "g" denotes parameters derived by geometric calculation. Then combination of Equations (1) and (3) gives the expected imbibition coefficient (C_g).

Experimentally measured imbibition coefficient (C_m), normalized by corresponding expected value (C_g), is plotted as a function of the pore radius (r_g) according to geometric calculation in Figure 3. It is reasonable to assume $\theta = 0°$ for hydrocarbons because of the superior oil adsorption ability. The contact angle for water is obtained by Equation (1) for imbibition into as-grown sponges under a constant electrode voltage of -1.0 V (versus Ag/AgCl in 3 KCl), which gives $\theta \sim 80°$. Note that r_g decreases with the compression ratio (α) according to Equation (3). When the compression is slight, C_m shows a good agreement with the prediction (C_g) based on simple geometric calculation. However, it is surprising to find that the derivation between C_m and C_g emerges as the increase of the compression degree (or the decrease of the geometric pore radius, r_g) for all three kinds of liquid. The stronger divergence of the experiment data for 1 M KOH is attributed to the relatively poor wettability of water on CNT surfaces even under potential control. The maximum C_m achieved experimentally here surpasses the expected C_g by around 120%, indicating the flow rate in compressed sponges has been significantly enhanced. This observation manifests liquid slippage on CNT surfaces during capillary filling of both oil and water in CNT sponges, which becomes more pronounced as the geometric radius
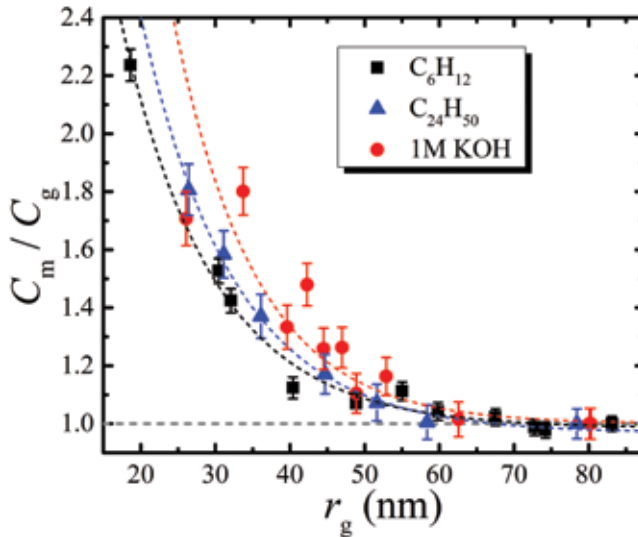

FIGURE 3
Imbibition coefficient versus geometric pore radius. The experimentally measured imbibition coefficient, C_m, normalized by the theoretical prediction, C_g, is plotted as a function of the geometric pore radius, r_g. Dots: experiment, Lines: exponential fitting for eye guide.

decreases. This is consistent with the recent demonstration of radius-dependent liquid slippage inside carbon nanotubes [17]. We remark the structure alteration of CNT sponges by compression may also influence the imbibition kinetics, for example, by changing the tortuosity besides effective pore radius. However, the tortuosity generally increases with the solid fraction of a fibrous media [34, 35], which, in fact, decreases the imbibition coefficient instead according to Equation (1), rather than the enhancement as observed in the present experiments.

In order to estimate the magnitude of slip length on CNT surfaces during capillary filling, we calculate the effective pore radius (r_m) by experimentally measured imbibition coefficient (C_m) according to Equation (1). Consider the CNT sponge as assembly of circular tubes of radius, r_g, and treat liquid flow in the channels as a Hagen-Poiseuille problem. Then the effective pore radius, r_m, for capillary filling is correlated with the geometric radius, r_g, by [10]

$$r_m = r_g + 4b,\tag{4}$$

where b is slip length. The resultant slip length (b) as a function of the geometric radius (r_g) is plotted in Figure 4. Consistent with the trend of the imbibition coefficient in Figure 3, slip length, b, also increases with the shrinkage of the pore size. A slip length of 18 nm is achieved when the geometric radius
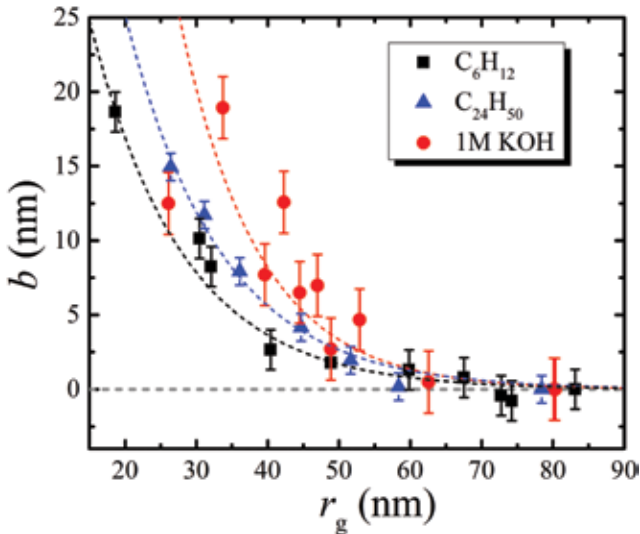

FIGURE 4
Pore-size dependence of liquid slippage. The graph shows the variation of the slip length (b) with geometric pore radius (r_g). Dots: experiment, Lines: exponential fitting for eye guide.

is around 20-30 nm for both organic liquid and water. The pore size-dependent slip length observed here is attributed to the reduction of interfacial friction between liquid and CNT surfaces, which is consistent with the observation in Ref. [17]. The relatively smaller magnitude may be due to the curvature dependence of liquid slippage on graphitic surfaces inside and outside the carbon nanotubes [14]. Although high shear rates may also induce slippage on solid surface, the shear rate in the present experiments (below 10^3 s^{-1}) is at least two order of magnitude smaller than required to produce similar slip effect on smooth hydrophobic surfaces [21, 36]. Thus, the dependence of liquid slippage on shear rate can be neglected here. In summary, it is seen that water slippage can happen on graphitic surfaces despite of surface wettability since the CNT surface has become hydrophilic by electrocapillary effects while the slip length magnitude may be reduced.

4 CONCLUSIONS

In summary, we have experimentally investigated the capillary filling of oil and water into CNT sponges with different compression degree using a gravimetric method. The classic Lucas-Washburn law is found to be well followed here in all the capillary filling processes. More importantly, we find that the imbibition rate in compressed sponges is accelerated for both oil and water, which is more pronounced for smaller pore size. The flow enhancement demonstrates liquid slippage on CNT surfaces during capillary flow in CNT sponges, which exhibits clear pore size dependence. The slip length reaches a magnitude of 20 nanometers, implying liquid slippage can also happen on wetting surfaces. The finding here contributes to the design of nanofluidic capillary system for (bio) chemical applications with high throughput.

5 ACKNOWLEDGEMENTS

REFERENCES

[1] Alava M., Dube M. and Rost M. Imbibition in disordered media. *Advances in Physics* **53** (2004), 83-175.

[2] Lauga E., Brenner M.P. and Stone H.A. Microfludics: the no-slip boundary condition. In Foss J., Tropea C. and Yarin A. (Eds.) *Handbook of Experimental Fluid Dynamics.* New York: Springer, 2005. **15**, pp. 1219-1240.

[3] Huber P., Soft matter in hard confinement: phase transition thermodynamics, structure, texture, diffusion and flow in nanoporous media. *Journal of Physics: Condensed Matter* **27** (2015), 103102.

[4] Washburn E.W. the Dynamics of capillary flow. *Physical Review* **17** (1921), 273-283.

[5] Lago M. and Araujo M. Capillary rise in porous media. *Journal of Physics A* **289** (2001), 1-17.

[6] Tas N.R., Haneveld J., Jansenm H.V., Elwenspoek M. and van den Berg A. Capillary filling speed of water in nanochannels. *Applied Physics Letters* **85** (2004), 3274-3276.

[7] Fries N. and Dreyer M. An analytic solution of capillary rise restrained by gravity. *Journal of Colloid Interface Science* **320** (2008), 259-263.

[8] Das S. and Mitra S.K. Different regimes in vertical capillary filling. *Physical Review E* **87** (2013), 063005.

[9] Gruener S., Hofmann T., Walacher D., Kityk A.V. and Huber P. Capillary rise of water in hydrophilic nanopores. *Physical Review E* **79** (2009), 067301.

[10] Vo T.Q., Barisik M. and Kim B. Near-surface viscosity effects on capillary rise of water in nanotubes. *Physical Review E* **92** (2015), 053009.

[11] Hummer G., Rasalah J.C. and Noworyta J.P. Water conduction through the hydrophobic channel of a carbon nanotube. *Nature* **414** (2001), 188-190.

[12] Majumder M., Chopra N., Andrews R. and Hinds B.J. Nanoscale hydrodynamics - enhanced flow in carbon nanotubes. *Nature* **438** (2005), 44-44.

[13] Holt J.K., Park H.G., Wang Y., Stadermann M., Artyukhin A.B., Grigoropoulos C.P., Noy A., Bakajin O. Fast mass transport through sub-2-nanometer carbon nanotubes. *Science* **312** (2006), 1034-1037.

[14] Falk K., Sedlmeier F., Joly L., Netz R.R. and Bocquet L. Molecular origin of fast water transport in carbon nanotube membranes: superlubricity *versus* curvature dependent friction. *Nano Letters.* **10** (2010), 4067-4073.

[15] Qin X., Yuan Q., Zhao Y., Xie S. and Liu Z. Measurement of the rate of water translocation through carbon nanotubes. *Nano Letters.* **11** (2011), 2173-2177.

[16] Ma M., Grey F., Shen L., Urbakh M., Wu S., Liu J.Z., Liu Y. and Zheng Q. Water transport inside carbon nanotubes mediated by phonon-induced oscillating friction. *Nature Nanotechnolgy* **10** (2015), 692-695.

[17] Secchi E., Marbach S., Nigues A., Stein D., Siria A. and Bocquet L. Massive radius-dependent flow slippage in carbon nanotubes. *Nature* **537** (2016), 210-213.

[18] Radha B., Esfandiar A., Wang F.C., Rooney A.P., Gopinadhan K., Keerthi A., Mishchenko A., Janardanan A., Blake P., Fumagalli L., Lozada-Hidalgo M., Garaj S., Haigh S.J., Grigorieva I.V., Wu H.A. and Geim A.K. Molecular transport through capillaries made with atomic-scale precision. *Nature* **538** (2016), 222-225.

[19] Cupelli C., Henrich B., Glatzel T., Zengerle R., Moseler M. and Santer M. Dynamic capillary wetting studied with dissipative particle dynamics. *New Journal of Physics* **10**(4) (2008), 043009.

[20] Joly L. Capillary filling with giant liquid/solid slip: dynamics of water uptake by carbon nanotubes. *Journal of Chemical Physics.* **135** (2011), 214705-214705-5.

[21] Choi C.-H., Johan K., Westin A. and Brener K.S. Apparent slip flows in hydrophilic and hydrophobic microchannels. *Physics of Fluids* **15** (2003), 2897-2902.

[22] Bonaccurso E., Kappl M. and Butt H.-J. Hydrodynamic force measurements: boundary slip of water on hydrophilic surfaces and electrokinetic effects. *Physical Review Letters.* **88** (2002), 076103.

[23] Lee K.P., Leese H. and Mattia D. Water flow enhancement in hydrophilic nanochannels. *Nanoscale* **4** (2012), 2621-2627.

[24] Sendner C., Horinek D., Bocquet L. and Netz R.R. Interfacial water at hydrophobic and hydrophilic surfaces: slip, viscosity and diffusion. *Langmuir* **25** (2009), 10768-10781.

[25] Ho T.A., Pavavassiliou D.V., Lee L. and Strioli A. Liquid water can slip on a hydrophilic surface. *Proceedings of the National Academy of Science U.S.A.* **108** (2011), 16170-16175.

[26] Dimitrov D.I., Milchev A. and Binder K. Capillary rise in nanopores: molecular dynamics evidence for the lucas-washburn equation. *Physical Review Letters* **99** (2007), 054501.

[27] Gui X., Wei J., Wang K., Cao A., Zhu H., Jia Y., Shu Q. and Wu D. Carbon nanotube sponges. *Advanced Materials* **22** (2010), 617-621.

[28] Xue Y., Yang Y., Sun H., Li X., Wu S., Cao A. and Duan H. A switchable and compressible carbon nanotube sponge electrocapillary imbiber. *Advanced Materials.* **27** (2015), 7241-7246.

[29] Li X., Xue Y., Zou M., Zhang D., Cao A. and Duan H. Direct oil recovery from saturated carbon nanotube sponges. *ACS Applied Materials and Interfaces* **8** (2016), 12337-12343.

[30] Wilhoit R.C., Marsh K.N., Hong X., Gadalla N. and Frenkel M. *Thermodynamic Properties of Organic Compounds and their Mixtures*. Berlin: Springer-Verlag, 2000.

[31] Xue Y., Markmann J., Duan H., Weissmuller J. and Huber P. Switchable imbibition in nanoporous gold. *Nature Communications.* **5** (2014), 4237.

[32] Gruener S., Sadjadi Z., Hermes H.E., Kityk A.V., Knorr K., Egelhaaf S.U., Rieger H. and Huber P. Anomalous front broadening during spontaneous imbibition in a matrix with elongated pores. *Proceedings of the National Academy of Science U.S.A.* **109** (2012), 10245-10250.

[33] Sruener S., Hermes H.E., Schillinger B., Egelhaaf S.U. and Huber P. Capillary rise dynamics of liquid hydrocarbons in mesoporous silica as explored by gravimetry, optical and neutron imaging: nano-rheology and determination of pore size distributions from the shape of imbibition fronts. *Colloids and Surfaces A* **496** (2016), 13-27.

[34] Ghanbarian B., Hunt A.G., Ewing R.P. and Sahimi M. Tortuosity in porous media: a critical review. *Soil Science Society of America Journal.* **77** (2012), 1461-1477.

[35] Vallabh R., Banks-Lee P. and Seyam A.-F. New approach for determining tortuosity in fibrous porous media. *Journal of Engineered Fibers and Fabrics* **5** (2010), 7-19.

[36] Martini A., Hsu H.-Y., Patankar N.A. and Lichter S. Slip at High shear rates. *Physical Review Letters* **100** (2008), 206001.